Effect of Architecture on the Micellar Properties of Amphiphilic Block Copolymers: Comparison of AB Linear Diblock, A^1A^2B, and A_2B Heteroarm Star Block Copolymers

Jongpil Yun and Rudolf Faust*

Polymer Science Program, Chemistry Department, University of Massachusetts, Lowell, Massachusetts 01854

László Sz. Szilágyi, Sándor Kéki, and Miklós Zsuga*

Department of Applied Chemistry, University of Debrecen, Egyetem tér 1 Debrecen H-4010, Hungary

Received October 24, 2002; Revised Manuscript Received December 13, 2002

ABSTRACT: Amphiphilic AB, A^1A^2B, and A_2B block copolymers, where A = polyisobutylene, B = poly(methyl vinyl ether), and the superscripts denote molecular weight asymmetry, with constant molecular weight and composition have been synthesized by living cationic polymerization. The influence of architecture on aqueous micellar properties of these block copolymers were investigated in the temperature range 20−30 °C by fluorescence spectroscopy and static and dynamic light scattering (SLS and DLS). The critical micelle concentration (cmc) measured at 23 °C increased in the order $A_2B < A^1A^2B <$ AB. The partition equilibrium constants, K_v of pyrene, characteristic of hydrophobicity, increased in the opposite order of cmc. The hydrodynamic radii (R_h) and aggregation numbers (N_{agg}) of micelles remained approximately constant in the whole temperature range for A^1A^2B and A_2B and below 25 °C for AB. At ∼25 °C, however, there was a sudden increase in both R_h and N_{agg} for AB. Below 25 °C both R_h and N_{agg} increased in the order $AB < A^1A^2B < A_2B$. The particle size distribution for all block copolymers remained narrow in the whole temperature range. The results are discussed in terms of possible morphologies.

Introduction

Above the critical micelle concentration (cmc) in dilute aqueous solutions, amphiphilic block copolymers, i.e., block copolymers consisting of hydrophobic and hydrophilic block segments, self-assemble into various aggregates, the most general being spherical micelles with a hydrophobic insoluble core and a hydrophilic shell. Micellization properties of amphiphilic block copolymers have attracted much attention due to their theoretical and practical interest.[1−4] The cmc, aggregation number, overall size, core, and shell dimensions are influenced by many factors such as chemical composition and molecular weight of the blocks,[5−12] solvent−polymer interactions, concentration, pH,[13] and temperature.[14,15] Recently, it was found that block copolymer architecture plays an important role in determining micellar properties.[16−24] In relation to our present work the report by Pispas et al.[18] is particularly important, as this was the first paper that reported micellization properties of A_2B miktoarm stars, consisting of polyisoprene (I) and polystyrene (S) as block segments, in comparison to the linear AB counterpart with the same molecular weight and composition. In *n*-decane, a selective solvent for polyisoprene, all samples formed spherical micelles. The aggregation number and hydrodynamic radii increased in the order $I_2S < S_2I <$ SI. The area of the core−corona interface per copolymer chain decreased in the order $I_2S > S_2I >$ SI although the difference between S_2I and SI was relatively small. Although the cmc could not be determined, it is apparent that the presence of a third arm changes the micellar properties considerably.

Further systematic studies of micellar properties as a function of architecture may help in the development of a general understanding of these systems. These studies demand model polymers with well-controlled molecular weight, narrow molecular weight distribution, and low compositional heterogeneity. Living polymerization techniques are eminently suitable to prepare these copolymers with complex architectures.[25−28] We have previously reported on the living cationic block copolymerization of isobutylene (IB) and methyl vinyl ether (MeVE) and published preliminary results on aqueous micellar properties of AB diblock and A_2B_2 type heteroarm star block copolymers, where A = polyisobutylene (PIB) and B = poly(methyl vinyl ether) (PMeVE).[29] The A_2B_2 star block copolymer exhibited a much higher cmc in comparison with a diblock copolymer of the same total M_n and composition or with the same segmental lengths. Above the cmc the average micelle size of A_2B_2 was also much larger than that obtained for AB with the same block lengths. Contrary to most published examples where one deals with frozen micelles due to the high T_g of the core forming polymer, PIB exhibits a T_g that is much lower than room temperature ($T_{g,PIB}$ = −73 °C),[29] and therefore the micelles should be in thermodynamic equilibrium with the dissolved unimers. In addition, PMeVE exhibits a lower critical solution temperature (LCST),[5] and therefore micellar properties may show an interesting temperature dependence. The properties of block copolymer micelles showing LCST behavior are also important from the practical point of view as they maybe utilized for thermosensitive targeted drug delivery.[30] This motivated us to start a systematic study on the effect of architecture on the micellization of other heteroarm star block copolymers of PIB (A) and PMeVE (B).

In a previous preliminary report, we presented a novel synthetic route for the synthesis of amphiphilic A_2B hetero-three-arm star block copolymers.[31] This synthetic

10.1021/ma021618r CCC: $25.00
Published on Web 02/01/2003

route is unique because the location of junction can be controlled. In this article, we report on the synthesis, characterization, and micellar properties of A_2B and A^1A^2B (where the superscripts denotes molecular weight asymmetry between PIB[1] and PIB[2]) heteroarm star block copolymers in reference to the corresponding linear AB block copolymer, with similar total M_n and composition.

Experimental Section

Materials. The syntheses of 2-chloro-2,4,4-trimethylpentane (TMPCl)[32] and 1,1-ditolylethylene (DTE)[33] have already been reported. 2-(Tributylstannyl)furan (2-Bu_3SnFu) (97%, Aldrich), titanium(IV) chloride ($TiCl_4$, 99.9%, Aldrich), and titanium(IV) isopropoxide ($Ti(OiPr)_4$, 99.999%, Aldrich) were used without further purification. 2,6-Di-*tert*-butylpyridine (DTBP) was vacuum-distilled over CaH_2. MeVE (98%, Aldrich) was purified by passing the gaseous monomer through a calcium hydride column and condensed under dry nitrogen atmosphere ([H_2O] < 1.0 ppm) in an Mbraun 150-M glovebox (Innovative Technology Inc.) at −80 °C. Hexanes (Hex) was purified as reported.[34] CH_2Cl_2 was washed with 10% aqueous sodium hydroxide to remove acidic impurities and washed with distilled water three times followed by drying over anhydrous sodium sulfate for 24 h at room temperature. Finally, the purified CH_2Cl_2 was refluxed over phosphorous pentoxide for 48 h and distilled just before use.

Representative Synthetic Procedure for Heteroarm Star Copolymers. All reactions were carried out in large (75 mL) test tubes under a dry ([H_2O] < 5 ppm) nitrogen atmosphere in an Mbraun 150-M glovebox (Innovative Technology Inc.). Living PIB^+ was prepared in Hex/CH_2Cl_2 (50/50 v/v) at −80 °C with TMPCl ([TMPCl] = 0.002 M) as initiator and $TiCl_4$ ([$TiCl_4$] = 0.036 M) as coinitiator, in the presence of a proton trap ([DTBP] = 0.003 M) at [IB] = 0.045 M. After 1 h polymerization, to the reactor containing living PIB^+, a stoichiometric amount of 2-PIB-Fu (M_n = 1250 g/mol, M_w/M_n = 1.2, prepared as described in ref 35) dissolved in CH_2Cl_2 was added to commence the coupling reaction. Upon the completion of the coupling reaction, $Ti(OiPr)_4$ ([$Ti(OiPr)_4$] = 0.0252 M) was added followed by the addition of MeVE (0.34 M), and the temperature was raised to 0 °C. After 15 h the polymerization was quenched with prechilled MeOH, and the solution was poured into excess 10% ammoniacal MeOH. Volatiles were allowed to evaporate under a hood, and the polymer was redissolved in CH_2Cl_2. The solution was filtered through a filter paper to remove inorganic salts, and the product was recovered by evaporation of the solvent. The crude products were purified by column chromatography on silica gel using Hex and THF as eluents.[36] The pure block copolymers were characterized by GPC and ^{1}H NMR spectroscopy.

Molecular Weight and Structural Analysis of the Copolymers. Molecular weights were measured at room temperature with a Waters HPLC system equipped with a model 510 HPLC pump, a model 410 differential refractometer, a model 441 UV−vis detector, an on-line multiangle laser light scattering (MALLS) detector (laser wavelength = 690 nm) (MiniDawn, Wyatt Technology Inc.), a model 712 sample processor, and five Ultrastyragel gel permeation chromatography (GPC) columns connected in the following series: 500, 10^3, 10^4, 10^5, and 100 Å. THF was used as a carrier solvent with a flow rate of 1 mL/min. Refractive index increments (dn/dc) of the block copolymers were calculated from the individual dn/dc of PMeVE (0.063)[37] and PIB (0.109)[38] in THF based on their relative compositions determined by ^{1}H NMR spectroscopy. ^{1}H NMR spectroscopy for structural analysis was carried out on a Bruker 250 MHz spectrometer using $CDCl_3$ (Cambridge Isotope Laboratories, Inc.) as a solvent.

Determination of Cmc. (A) Surface Tension Measurements. Surface tensions were measured with a SensaDyne 6000 surface tensiometer (Chem-Dyne Research Co.) using the maximum bubble pressure method at a bubble rate of 1/s with nitrogen as an inert gas. Data were collected on a personal computer and analyzed using SensaDyne 6000 software (Chem-Dyne Research Co.).

Table 1. Molecular Weights and Composition of the Block Copolymers

block copolymers	M_n (g/mol)	M_n of A block (g/mol)	M_n of B block (g/mol)	M_w/M_n	dn/dc[a] (mL/g)
AB	17 800	2800	15 000	1.02	0.149
A^1A^2B	17 600	1800^1, 800^2	15 000	1.13	0.149
A_2B	16 500	1250, 1250	14 000	1.13	0.131

[a] The dn/dc values were determined in water at 25 °C.

(B) Fluorescence Measurements. Fluorescence measurements were performed using a luminescence spectrometer LS55 (Perkin Elmer Instrument.) with a thermostated cell. Pyrene was used as fluorescence probe. 1 mL of pyrene solution in THF (1.2×10^{-3} M) was added to 1 L of distilled water. THF was removed by a rotary evaporator at 30 °C for 2 h, and resulting pyrene solution in water (1.2×10^{-6} M) was mixed with block copolymer solution. The pyrene concentration in block copolymer solution was 6.0×10^{-7} M. For the measurements of pyrene excitation spectra scan speed and accumulation scan numbers were set at 100 nm/min and 5, respectively.

(C) Light Scattering Measurements. The number of scattered photons was monitored with a Brookhaven light scattering instrument at $\Theta = 90°$ detector angle. The cmc's were determined from the scattered light intensity vs concentration plots as a threshold concentration at which the scattered light intensity started to increase.

Observation of Cloud Points. A polymer solution (10 mL in a 20 mL glass scintillation vial) with a concentration of 0.05 mg/mL was slowly heated in a water bath. The cloud point was observed visually.

Sample Preparation for Cmc and Laser Light Scattering Measurements. Stock solutions were prepared by dissolving the block copolymer samples in distilled water, filtered through 0.45 μm membrane filter, under stirring. From the stock solution a series of concentration was prepared by dilution. Especially for the light scattering measurement, the solutions were filtered through 1 μm membrane filter and were allowed to stand overnight at a given temperature (20−30 °C) to equilibrate.

Characterization of Micelles. Static and Dynamic Light Scattering. DAWN EOS (Waytt Technology) multiangle static light scattering (SLS) instrument operating at 690 nm was employed to determine the weight-average molecular weight (M_w) of the micelles using the Zimm plot in the concentration range 0.02−0.08 mg/mL

$$Kc/\Delta R(\Theta,c) = (1/M_w)(1 + (R_g^2 q^2)/3) + 2A_2c$$

where the optical constant K is defined by $K = 4\pi^2 n^2 (dn/dc)^2/(N_A \lambda_i^4)$, with n being the refractive index of solvent, N_A the Avogadro's number, dn/dc the refractive index increment, and λ_i the wavelength of the incident beam in vacuum, and the scattering vector q is given by $q = (4\pi n/\lambda_i)\sin(\Theta/2)$. R_g and A_2 are the radius of gyration and the second virial coefficient, respectively.

The refractive index increments (dn/dc) of block copolymers in water, listed in Table 1, were determined at 25 °C with an OPTILAB DSP (Wyatt Technology) refractometer at a wavelength of 690 nm.

For the dynamic light scattering (DLS) experiments a Brookhaven light scattering instrument equipped with a BI-9000 digital correlator and temperature controlled goniometer was used. The light source was a solid-state vertically polarized laser working at 533.4 nm. The hydrodynamic radii (R_h) of micelles were determined from the characteristic decay rate ($\langle\Gamma\rangle$) of the autocorrelation function of the scattered light intensity at 90° using the methods of cumulants. The diffusion coefficient (D) was calculated as $D = \langle\Gamma\rangle/q^2$ where q is the scattering vector. Since no significant change of D in the concentration range of 0.001−0.1 mg/mL was observed, the

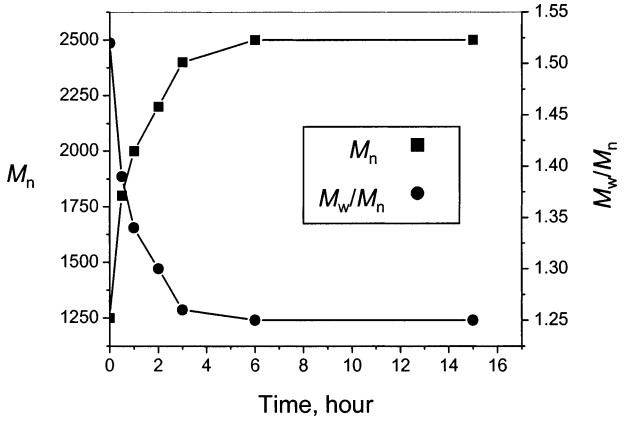

Figure 1. M_n and M_w/M_n for coupling reaction of living PIB^+ and 2-PIB-Fu. Reaction conditions: [TMPCl] = 0.002 M, [$TiCl_4$] = 0.036 M, [DTBP] = 0.003 M, [IB] = 0.045 M (M_n = 1250, M_w/M_n = 1.52), [2-PIB-Fu] = 0.002 M (M_n = 1250, M_w/M_n = 1.2), Hex/CH_2Cl_2 (40/60 v/v) at −80 °C.

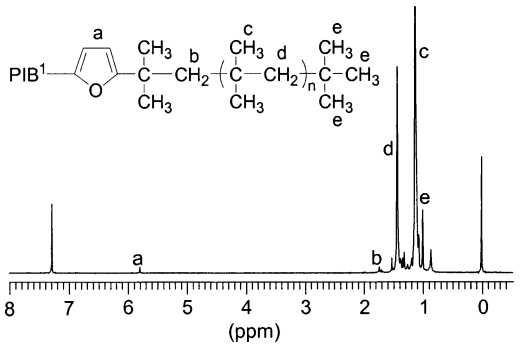

Figure 2. ^{1}H NMR spectrum of PIB^1-Fu-PIB^2 in $CDCl_3$ (PIB^1 (M_n = 1250), PIB^2 (M_n = 1250)).

samples at a concentration of 0.05 mg/mL were used. R_h was obtained using the Stokes−Einstein relation given by $R_h = kT/(6\pi\eta D)$, where k, T, and η are the Boltzmann constant, the temperature, and the viscosity of the solvent, respectively. The particle size distribution was evaluated by the nonnegative constraint least-squares (NNLS) method. The polydispersity of the micelles is represented as μ_2/Γ^2, where μ_2 is the second cumulant of the decay function.

Results and Discussion

Synthesis and Characterization. The AB diblock copolymer was synthesized by sequential monomer addition according to a previous report,[33] involving the capping of living PIB with DTE and tuning the Lewis acidity before the introduction of MeVE. The A_2B and A^1A^2B heteroarm star block copolymers were prepared according to Scheme 1, reported previously.[31] First, living PIB^+ is prepared in Hex/CH_2Cl_2 (50/50, v/v) at −80 °C in conjunction with $TiCl_4$. Upon complete monomer conversion, a stoichiometric amount of 2-PIB-Fu is added to the reactor, simultaneously increasing the polarity to Hex/CH_2Cl_2 (40/60, v/v). To monitor the coupling reaction, aliquots of the reaction mixture were withdrawn from the reactor at various times and quenched with prechilled methanol, and the samples were analyzed by ^{1}H NMR spectroscopy and GPC. As shown in Figure 1, the coupling reaction is complete in 6 h.

The ^{1}H NMR spectrum of the final product in Figure 2 shows that the three resonance signals (6.0, 6.3, and 7.4 ppm) due to the nonequivalent protons on the furanyl ring in 2-PIB-Fu completely disappeared, and

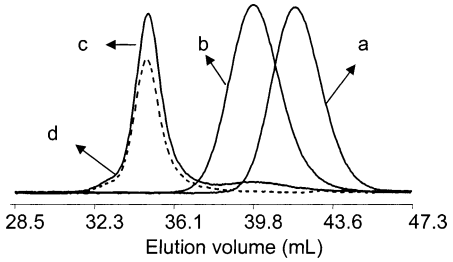

Figure 3. Overlaid GPC chromatograms of (a) precursor 2-PIB-Fu (M_n = 1250, M_w/M_n = 1.20), (b) coupled PIB (M_n = 2500, M_w/M_n 1.25), (c) crude A_2B (M_n = 11 000, M_w/M_n = 1.20), and (d) purified A_2B (M_n = 16 500, M_w/M_n = 1.13). Reaction conditions: [living PIB^+] = 0.002 M, (M_n = 1250, M_w/M_n = 1.52) [$TiCl_4$] = 0.036 M, [DTBP] = 0.003 M, [MeVE] = 0.34 M, [2-PIB-Fu] = 0.002 M (M_n = 1250, M_w/M_n = 1.2), Hex/CH_2Cl_2 (40/60 v/v) at 0 °C.

Scheme 1

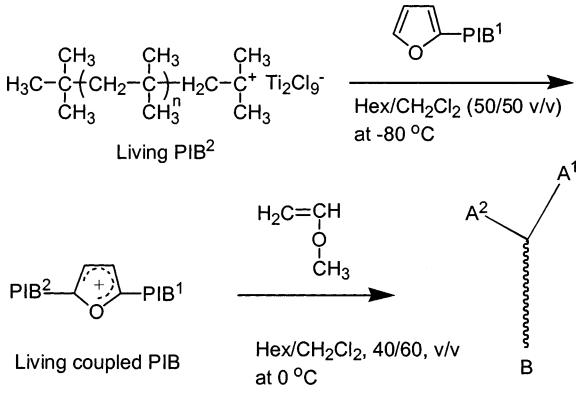

a single signal appeared at 5.8 ppm attributed to two chemically equivalent protons on the furanyl ring.

GPC traces of the original 2-PIB-Fu and coupled PIB are shown in Figure 3. The coupled product exhibited approximately the sum of the molecular weights of the precursor 2-PIB-Fu and PIB^+ and lower polydispersity index (PDI), indicating quantitative coupling reaction.

After successful coupling has been achieved, the polymerization of MeVE was investigated according to Scheme 1. The coupling reaction was followed by the addition of $Ti(OiPr)_4$ ([$Ti(OiPr)_4$]/[$TiCl_4$] = 0.7) to reduce the Lewis acidity, which is optimal for the polymerization of MeVE.[35] After tuning the Lewis acidity, MeVE was introduced to the reactor followed by the increase of temperature to 0 °C to accelerate the polymerization of MeVE. As the polymerization proceeded, the transparent yellow color of the solution, which developed upon addition of 2-PIB-Fu due to the generation of stable carbenium ion on the furanyl ring, gradually vanished. After 15 h, the polymerization was quenched with prechilled methanol (conversion of MeVE ∼ 90%). The GPC RI trace (Figure 3) of the crude A_2B shows a hump at higher elution volume, which indicates that the crude product contains star block copolymers as well as unreacted coupled PIB. The crude product was purified by column chromatography to obtain pure A_2B. The crossover efficiency was approximately 63% as determined from the weights of the fractions. The ^{1}H NMR spectrum of the separated, homo-PIB was identical to that of the product obtained in the coupling reaction. The relatively low crossover efficiency has been explained in our previous report by the steric crowding at the actual site of initiation at C-4 on the furanyl ring.[35]

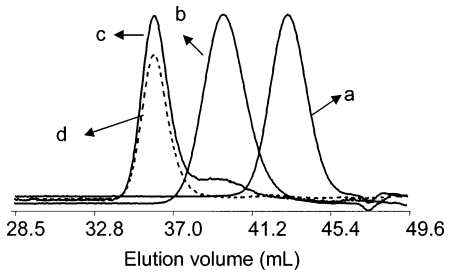

Figure 4. Overlaid GPC chromatograms of (a) precursor 2-PIB-Fu (M_n = 800, M_w/M_n = 1.25), (b) coupled PIB (M_n = 2600, M_w/M_n = 1.30), (c) crude A^1A^2B (M_n = 13 000, M_w/M_n = 1.22), and (d) purified A^1A^2B (M_n = 17 600, M_w/M_n = 1.13). Reaction conditions: [living PIB^+] = 0.002 M, (M_n = 1800, M_w/M_n = 1.52), [$TiCl_4$] = 0.036 M, [DTBP] = 0.003 M, [MeVE] = 0.34 M, [2-PIB-Fu] = 0.002 M (M_n = 800, M_w/M_n = 1.25), Hex/CH_2Cl_2, (40/60, v/v) at 0 °C.

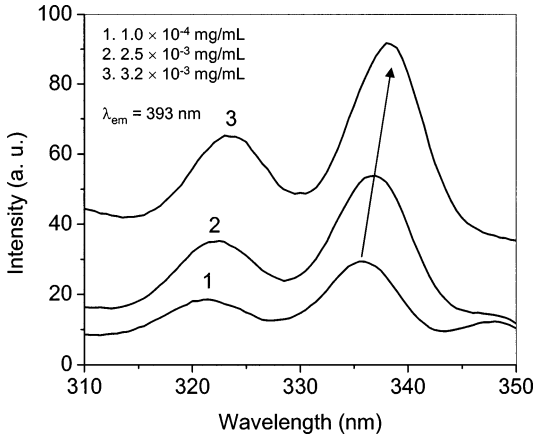

Figure 5. Excitation spectra of pyrene as a function of A^1A^2B block copolymer concentration in water at 23 °C.

Scheme 2. Illustration of Block Copolymer Architectures

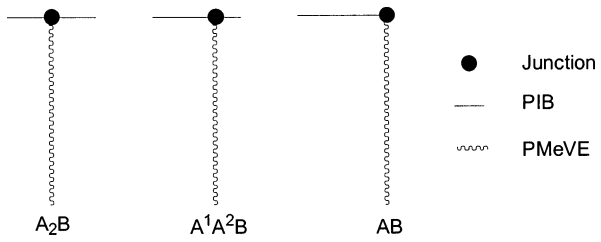

A^1A^2B was prepared by a similar procedure to that of A_2B. Figure 4 shows the GPC RI traces of A^1, the coupled A^1A^2, and the crude and purified A^1A^2B.

As can be seen in Scheme 2, the M_n of hydrophobic and hydrophilic segment length was kept constant in the three block copolymers (AB, A^1A^2B, A_2B), while the location of junction was varied. The overall composition (∼15 wt % PIB, ∼85 wt % PMeVE) was designed to provide water-soluble products.[33] The molecular weight and compositions are summarized in Table 1.

Characterization of Micelles. Effect of Architecture on Cmc. The onset of micelle formation (cmc) in water was determined by light scattering measurements and fluorescence spectroscopy using pyrene as a fluorescence probe.[39] Above the cmc pyrene molecules partition into the hydrophobic core of the micelles. Thus, their photophysical characteristics change compared to pyrene molecules in water. In Figure 5, the excitation spectra of pyrene are shown at various block copolymer concentrations.

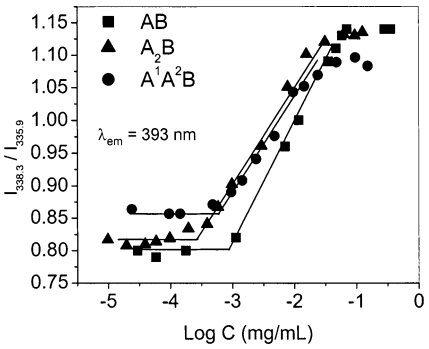

Figure 6. Plot of $I_{338.3}/I_{335.9}$ (from pyrene excitation spectra) vs log C for A_2B, A^1A^2B, and AB at 23 °C.

Table 2. Cmc and K_v of Block Copolymers

block copolymers	cmc × 10^3 (mg/mL)[a]	cmc × 10^2 (mg/mL)[b]	χ_{PIB}[c]	$K_v \times 10^{-6}$ [d]
AB	1.0	1.10	0.16	1.02
A^1A^2B	0.56	0.12	0.15	1.12
A_2B	0.32	0.11	0.15	1.87

[a] Measured by the fluorescence technique at 23 °C. [b] Measured by light scattering at 23 °C. [c] Weight fraction of polyisobutylene. [d] Determined at 23 °C.

Above a critical concentration a shift of pyrene spectra from 335.9 to 338.3 nm is observed, indicating partitioning of pyrene into the hydrophobic micellar core. This shift was utilized to determine the cmc values. The fluorescence intensity ratios ($I_{338.3}/I_{335.9}$) of pyrene excitation spectra vs the logarithm of various block copolymer concentrations are plotted in Figure 6.

A substantial increase of the intensity ratio was detected at a certain concentration, indicating the onset of micelle formation. The cmc was determined from the intersection of the two straight lines in Figure 6. The cmc values (Table 2) are in the range of M (3.16×10^{-4}–1.0×10^{-3} mg/mL), comparable to other polymeric amphiphiles based on PIB as a hydrophobic block.[40] The cmc values obtained from light scattering are also listed in Table 2.

The difference in cmc values determined by fluorescence spectroscopy and light scattering can be attributed to the different sensitivity of the two methods as reported elsewhere.[39] Both methods, however, yielded cmc's that increased in the order $A_2B < A^1A^2B <$ AB. We have also applied a technique employed by us earlier to determine cmc based on surface tension measurements using the maximum bubble pressure method at a bubble rate of 1/s. Although the $A_2B < A^1A^2B <$ AB trend was the same, this method provided cmc's that were 2−3 orders of magnitude higher than values obtained by light scattering. Apparently, diffusion of block copolymers to the gas/liquid interface is slow, and static surface tension by the bubble method may not be attained especially when surface generation is rapid. Thus, we note in this paper that the measurement of surface tension may not be suitable to determine cmc of amphiphilic block copolymers. The effect of temperature on cmc for AB was also investigated. The cmc decreased from 1.1×10^{-2} at 20 °C to 1.0×10^{-3} mg/mL at 30 °C, which is typical in entropy-driven micellization of block copolymers in aqueous solution.

Partitioning of Pyrene to Core of Micelle. The method of Wilhelm et al.[39] can be used to calculate the partition equilibrium constant K_v, characteristic of the hydrophobicity of the micellar core. K_v of pyrene was

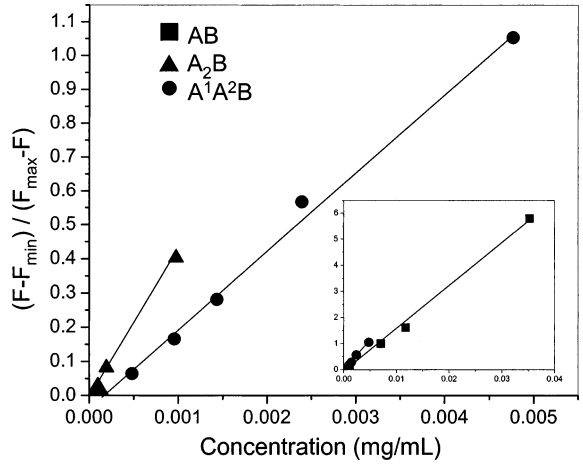

Figure 7. Plots of $(F - F_{min})/(F_{max} - F)$ vs concentration of block copolymers at 23 °C.

calculated by considering the incorporation of pyrene into the micelles as a simple equilibrium between the micellar phase and the aqueous phase. Thus, the ratio of pyrene concentration in the micellar to the aqueous phase ($[Py]_m/[Py]_w$) can be correlated to the volume ratio of each phase according to eq 1.

$$[Py]_m/[Py]_w = K_v V_m/V_w \quad (1)$$

Equation 1 can be rewritten as

$$[Py]_m/[Py]_w = K_v \chi c/ 1000\rho \quad (2)$$

where χ is the weight fraction of hydrophobic PIB block, c is the concentration of the block copolymer, and ρ is the density of the PIB micellar core, assumed to have the same value as that of bulk PIB (1.0 g/mL). $[Py]_m/[Py]_w$ can be written as[39]

$$[Py]_m/[Py]_w = (F - F_{min})/(F_{max} - F) \quad (3)$$

where F_{min} and F_{max} correspond to the average magnitude of $I_{338.3}/I_{335.9}$ in the flat region of low and high concentration ranges and F is the $I_{338.3}/I_{335.9}$ intensity ratio in the intermediate concentration range of the block copolymers. By combining eqs 2 and 3, K_v was determined from the slope of the linear line by plotting $(F - F_{min})/(F_{max} - F)$ against block copolymer concentrations above cmc (Figure 7).

The K_v values for AB, A^1A^2B, and A_2B are summarized in Table 2. K_v (and thus the hydrophobicity) increase in the opposite order of cmc, which is in line with expectations and with other reports.[6,41,42] Thus, it seems that the protection of hydrophobic A chain by the hydrophilic B chain is less efficient when A is branched. In other words, a branched hydrophopic A chain displays properties of a nonbranched linear chain of higher molecular weight.

Effect of Architecture on Micellar Dimensions. The effect of the junction location on M_w, N_{agg}, and R_h was investigated by SLS and DLS in the temperature range from 20 to 30 °C. As shown in Figures 8 and 9, below 25 °C R_h and N_{agg} increase in the order AB < A^1A^2B < A_2B. A representative plot of Kc/R vs concentration is shown in Figure 10.

According to our finding, the block copolymer with lower cmc has a greater tendency to form micelles, which results in greater N_{agg} and R_h. A sudden and significant increase in R_h and N_{agg} was observed with

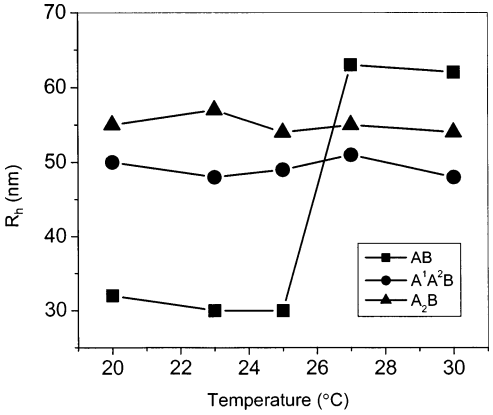

Figure 8. R_h of the micelles formed from A_2B, A^1A^2B, and AB vs temperature.

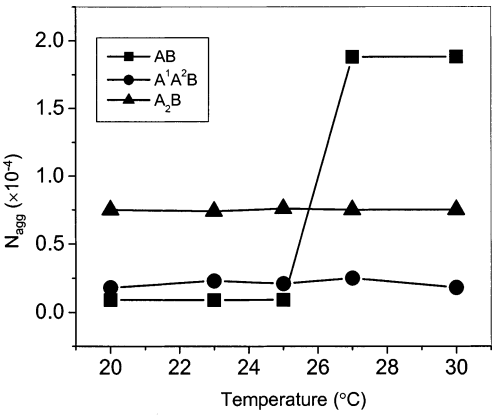

Figure 9. N_{agg} of the micelles formed from A_2B, A^1A^2B, and AB vs temperature.

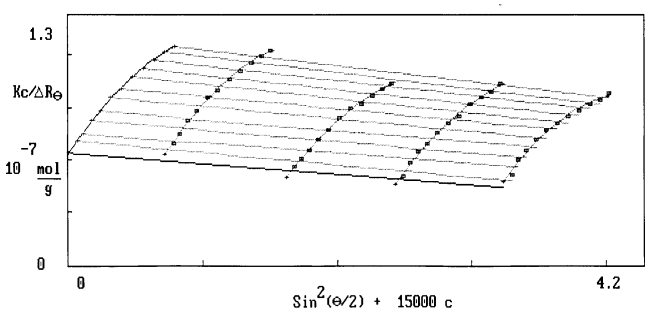

Figure 10. Zimm plot analysis of the micelles formed from AB at 23 °C. The range of concentration is 0.02−0.08 mg/mL.

AB diblock at 25 °C, while the corresponding values for A^1A^2B and A_2B remained approximately constant. The size distributions remained monomodal and narrow in the whole temperature range. PMeVE is known to exhibit a lower critical solution temperature behavior.[5] Thus, with the increase of temperature the B segment becomes less soluble, and this results in the formation of larger aggregates. The temperature where the aggregation of AB micelles was observed, however, is below the cloud point, which was observed at 33 °C. Interestingly, micelles formed from A^1A^2B and A_2B do not show this temperature dependence, and the cloud point for A^1A^2B and A_2B was not observed up to 50 °C. We propose that the sudden and significant increase in R_h and N_{agg} observed with AB diblock at 25 °C is due to a temperature-induced morphological change (micelles to aggregates or micelles to vesicles, see later) brought about by the decrease of hydrophilicity of the corona. Since the branched A is more hydrophobic than the

Table 3. Characterization of Micelles from Block Copolymers below 25 °C

block copolymers	$M_w \times 10^{-7}$ (g/mol)	N_{agg}	R_h (nm)	R_g/R_h	μ_2/Γ^2
AB	1.63	900	31	1.03	0.055
A^1A^2B	4.18	2100	49	1.12	0.033
A_2B	14.0	7500	55	0.96	0.016

Table 4. Geometrical Parameters for the Micelles Formed from AB, A^1A^2B, and A_2B Block Copolymers

block copolymers	R_c (nm)	S (nm)	A_c (nm^2)	$A_{c,N}$ (nm^2)	C_r
AB	10.0	21.0	1256	1.40	3.1
A^1A^2B	13.0	36.0	2123	1.01	1.8
A_2B	19.5	35.5	4776	0.64	1.7

linear A, heteroarm star block copolymers A^1A^2B and A_2B form aggregates or vesicles even below 25 °C and do not show the above phenomenon.

The average values of M_w, N_{agg}, and R_h along with values of R_g/R_h and μ_2/Γ^2 for temperatures below 25 °C are listed in Table 3. The M_w's and correspondingly the N_{agg} values, which range from 900 to 7500, are much higher, especially for A^1A^2B and A_2B, than generally reported for block copolymer micelles. For instance, aggregation numbers of ~150 have been reported by Schuch et al.[40] for poly(isobutylene-*b*-methacrylic acid) block copolymers with similar total molecular weights (albeit different hydrophobic/hydrophilic composition) to ours. Large aggregation numbers (N_{agg} = 2430) and correspondingly large micelle dimensions (R_h = 33.9 nm), similar to ours, however, have been reported with poly(ethylene-*co*-propylene)-*block*-poly(ethylene oxide) with an overall molecular weight (M_n = 11 100).[43] Despite the large R_h and N_{agg}, the micelles were spherical in shape and consisted of a hydrophobic core and a highly swollen hydrophilic corona. The high R_h and N_{agg} values were explained by the large interfacial tension between water and poly(ethylene-*co*-propylene). This explanation may also hold in our system.

When R_h exceeds the contour length of the polymer chain, it is rational to suggest micellar aggregates, e.g., vesicles, such as in the case of polybutadiene-*block*-poly(L-glutamate) of certain compositions, recently reported by Kukula et al.[44] In our case, however, it is not possible to establish the nature of micelles or micellar aggregates based only on M_w, N_{agg}, and R_h in Table 3. Therefore, we calculated other micellar parameters (see Table 4) by assuming spherical core−shell type micelles. Unreasonable values would indicate that our model is in fact wrong and that micellar aggregates, e.g., vesicles, are present. The R_g/R_h value is useful to charaterize micellar shape. For homogeneous hard spheres R_g/R_h = 0.775.[45] Experimental values of R_g/R_h for spherical micelles of flexible polymers, however, are usually in the range 0.8−1.3.[40,45] In our case the R_g/R_h ratios are similar for all three block copolymers, and the $R_g/R_h \sim 1$ value is consistent with (a) spherical micelles or aggregates of micelles and (b) vesicles.

For individual micelles with a core−shell structure, the radius of the core (R_c) can be calculated using eq 4[18,46]

$$R_c = [3M_{w,mic}w_{PIB}/(4\pi N_A \rho_{PIB}\Phi_{PIB})]^{1/3} \quad (4)$$

where $M_{w,mic}$ is the weight-average molecular weight of micelle, w_{PIB} the weight fraction of PIB in the copolymer, N_A Avogadro's number, ρ_{PIB} the density of PIB, and Φ_{PIB} the volume fraction of PIB in the core of micelle. Using the values of ρ_{PIB} = 1 g/mL[47] and Φ_{PIB} = 1, one can calculate the R_c. The thickness of the shell (S) can also be calculated from the difference of R_h and R_c, i.e., $S = R_h - R_c$. The area of the core (A_c) and the area per PMVE chain at the PIB interface ($A_{c,N}$) can be calculated by eqs 5 and 6, respectively.

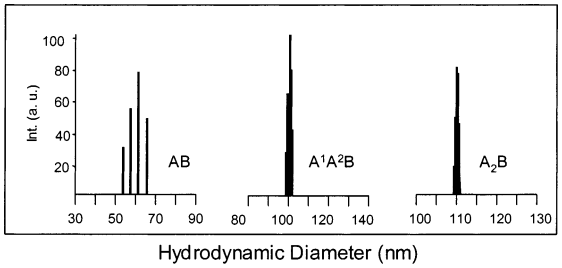

Figure 11. Size distribution of block copolymers at 23 °C.

$$A_c = 4\pi R_c^2 \quad (5)$$

$$A_{c,N} = 4\pi R_c^2/N_{agg} \quad (6)$$

One can also calculate the coiling ratio (C_r) of the PMVE segment in the shell of the micelles as

$$C_r = DP_n L/S \quad (7)$$

where DP_n is the number-average degree of polymerization of PMeVE, S is the thickness of shell, and L is the length of monomeric unit of methyl vinyl ether ($L \sim 0.25$ nm).[48] The geometrical parameters for the micelles formed from AB, A^1A^2B, and A_2B block copolymers using the results of static and dynamic light scattering are summarized in Table 4.

According to the data of Table 4, R_c increases in the order AB < A^1A^2B < A_2B. This is logical since the aggregation number increases in the same order. The calculated area per PMeVE chain decreases in the order AB > A^1A^2B > A_2B. The shell thickness is similar for A^1A^2B and A_2B; however, S is much smaller for AB. When C_r is similar, the shell thickness is usually the function of the length of the shell-forming block, which is constant in our case. The area per PMeVE chains and therefore C_r, however, are not constant, and the thickness of the shell increases in the order AB < $A^1A^2B \approx A_2B$ order. From the simple point of view that a junction at the interface usually introduces a bending of the curvature away from the junction, one could have predicted the opposite trend.

It should be noted that in our case the values of $A_{c,N}$ are much smaller than those reported for micelles formed from other block copolymers;[18,48] i.e., the PMeVE chains are highly stretched. This and other considerations discussed above lead us to conclude that at least for A^1A^2B and A_2B we are dealing with micellar aggregates or vesicles in which the structural arrangement of the hydrophilic segments are more favorable. Micellar clusters tend to form from "crew-cut micelles", i.e., micelles where the core is much larger than the corona. In our case, however, the core is much smaller than the corona ("hairy micelles"). According to Figure 11 and the μ_2/Γ^2 ratio listed in Table 3, the size distributions of micelles obtained for all three copolymers are monomodal and narrow. This would also suggest regular superstructures, e.g., vesicles, since multimicellar aggregates might be expected to exhibit a broader size

distribution (PDI > 0.05).[49] A similar argument was used by Schuch et al.[40] to explain the presence of large structures, presumably vesicles, with narrow size distribution. Chang et al.,[50] however, recently reported large aggregates of micelles that retained a relatively narrow size distribution. Therefore, future work will aim at visual identification of the micellar superstructures.

Conclusions

Micellar properties of block copolymers are strongly influenced by polymer architecture. Even a relatively simple change such as change in the location of a junction in AB, A_2B, and A^1A^2B type block copolymers results in different cmc, R_h, and N_{agg} values. The cmc values, which increase in the order $A_2B < A^1A^2B < AB$, as well as the partition equilibrium constants of pyrene, which change in the opposite order suggest that a branched A segment is more hydrophobic than a linear one. This is also corroborated by R_h and N_{agg}, which increased in the order $AB < A^1A^2B < A_2B$ below 25 °C. The large aggregation numbers and the resulting large micellar dimensions suggest vesicular structures, which will be examined in future research.

Acknowledgment. Financial support from the National Science Foundation (DMR-9806418 and INT-0099682) and from the Hungarian Academy of Sciences (MTA-OTKA-NSF) No. 62 and from OTKA No. T037448 and the Bolyai Janos Fellowship is gratefully acknowledged. We also thank the Center for Advanced Materials for assistance with the fluorescence measurements.

References and Notes

(1) Gref, R.; Minamitake, Y.; Peracchia, M. T.; Trubetskoy, V.; Torchilin, V.; Langer, R. *Science* **1994**, *263*, 1600.
(2) Wilhelm, M.; Zhao, C. L.; Wang, Y.; Xu, R.; Winnik, M. A.; Mura, J. L.; Riess, G.; Croucher, M. D. *Macromolecules* **1991**, *24*, 1033.
(3) Xu, R.; Winnik, M. A.; Riess, G.; Chu, B.; Croucher, M. D. *Macromolecules* **1992**, *25*, 644.
(4) Yu, K.; Eisenberg, A. *Macromolecules* **1996**, *29*, 6359.
(5) Forder, C.; Patrickios, C. S.; Armes, S. P.; Billingham, N. C. *Macromolecules* **1996**, *29*, 8160.
(6) Lee, S. C.; Chang, Y.; Yoon, J. S.; Kim, C.; Kwon, I. C.; Kim, Y. H.; Jeong, S. Y. *Macromolecules* **1999**, *32*, 1847.
(7) Tanodekaew, S.; Deng, N. J.; Smith, S.; Yang, Y. W.; Attwood, D.; Booth, C. *J. Phys. Chem.* **1993**, *97*, 11847.
(8) Yu, G. E.; Ameri, M.; Yang, Z.; Attwood, D.; Price, C.; Booth, C. *J. Phys. Chem. B* **1997**, *101*, 4394.
(9) Nace, V. M. *J. Am. Oil Chem. Soc.* **1996**, *73*, 1.
(10) Yang, Z.; Pickard, S.; Deng, N. J.; Barlow, R. J.; Attwood, D.; Booth, C. *Macromolecules* **1994**, *27*, 2371.
(11) Zhang, L.; Eisenberg, A. *J. Am. Chem. Soc.* **1996**, *118*, 3168.
(12) Thurmond, II, K. B.; Kowalewski, T.; Wooley, K. L. *J. Am. Chem. Soc.* **1997**, *119*, 6656.
(13) Gohy, J. F.; Varshney, S. K.; Jérôme, R. *Macromolecules* **2001**, *34*, 3361.
(14) Stam, J. V.; Creutz, S.; De Schryver, F.; Jérôme, R. *Macromolecules* **2000**, *33*, 6388.
(15) Kikuchi, A.; Nose, T. *Macromolecules* **1996**, *29*, 6770.
(16) Voulgaris, D.; Tsitsilianis, C.; Grayer, V.; Esselink, F. J.; Hadziioannou, G. *Polymer* **1999**, *40*, 5879.
(17) Voulgaris, D.; Tsitsilianis, C.; Esselink, F. J.; Hadziioannou, G. *Polymer* **1998**, *39*, 6429.
(18) Pispas, S.; Hadjichristidis, R.; Potemkin, I.; Khokhlov, A. *Macromolecules* **2000**, *33*, 1741.
(19) Tsitsilianis, C.; Alexandridis, P.; Lindman, B. *Macromolecules* **2001**, *34*, 5979.
(20) Sotiriou, K.; Nannou, A.; Velis, G.; Pispas, S. *Macromolecules* **2002**, *35*, 4106.
(21) Tsitsilianis, C.; Voulgaris, D.; Stepanek, M.; Podhajecka, K.; Prochazka, K.; Tuzar, Z.; Brown, W. *Langmuir* **2000**, *16*, 6868.
(22) Hadjichristidis, N.; Poulos, Y.; Pispas, S. *Macromolecules* **1998**, *31*, 4177.
(23) Voulgaris, D.; Tsitsilianis, C. *Macromol. Chem. Phys.* **2001**, *202*, 3284.
(24) Tsitsilianis, C.; Voulgaris, D.; Kosmas, M. *Polymer* **1998**, 39, 3571.
(25) Miayamoto, M.; Sawamoto, M.; Higashimura, T. *Macromolecules* **1984**, *17*, 265.
(26) Faust, R.; Kennedy, J. P. *Polym. Bull.* **1986**, *15*, 317; *J. Polym. Sci., Polym. Chem. Ed.* **1987**, *A25*, 1847.
(27) Szwarc, M. *Nature (London)* **1956**, *178*, 1168.
(28) Szwarc, M.; Levy, M.; Milkovich, R. *J. Am. Chem. Soc.* **1956**, *78*, 2656.
(29) Bae, Y. C.; Faust, R. *Macromolecules* **1998**, *31*, 2480.
(30) Kohori, F.; Sakai, K.; Aoyagi, T.; Yokyama, M.; Sakurai, Y.; Okano, T. *J. Controlled Release* **1998**, *55*, 87.
(31) Yun, J.; Faust, R. *Polym. Prepr.* **1999**, *40* (2), 1041.
(32) Fodor, Z.; Gyor, M.; Wang, H. C.; Faust, R. *J. Macromol. Sci., Pure Appl. Chem.* **1993**, *A30*, 349.
(33) Hadjikyriacou, S.; Faust, R. *Macromolecules* **1996**, *29*, 5261.
(34) Hadjikyriacou, S.; Faust, R. *Macromolecules* **2000**, *33*, 730.
(35) Hadjikyriacou, S.; Faust, R. *Macromolecules* **1999**, *32*, 6393.
(36) Perneker, T.; Kennedy, J. P. *Polym. Bull.* **1992**, *29*, 27.
(37) Cotts, D. B. *J. Polym. Sci., Polym. Phys. Ed.* **1983,** *21*, 1381.
(38) Chance, R. R.; Baniukiewicz, S. P.; Mintz, D.; Ver Strate, G.; Hadjichristidis, N. *Int. J. Polym. Anal. Charact.* **1995**, *1*, 3.
(39) Wilhelm, M.; Zhao, C. L.; Wang, Y.; Xu, R.; Winnik, M. A.; Mura, J. L.; Riess, G.; Croucher, M. D. *Macromolecules* **1991**, *24*, 1033.
(40) Schuch, H.; Klingler, J.; Rossmanith, P.; Frechen, T.; Gerst, M.; Feldthusen, F.; Müller, A. H. E. *Macromolecules* **2000**, *33*, 1734.
(41) Kim, C.; Lee, S. C.; Kown, I. C.; Chung, H.; Jeong, S. Y. *Macromolecules* **2002**, *35*, 193.
(42) Kim, C.; Lee, S. C.; Shin, J. H.; Yoon, J. S.; Kown, I. C.; Jeong, S. Y. *Macromolecules* **2000**, *33*, 7448.
(43) Poppe, A.; Willner, L.; Allgaier, J.; Stellbrink, J.; Richter, D. *Macromolecules* **1997**, *30*, 7462.
(44) Kukula, H.; Schlaad, H.; Antonietti, M.; Foerster, S. *J. Am. Chem. Soc.* **2002**, *124*, 1658.
(45) Yamakawa, H. *Modern Theory of Polymer Solutions*; Harper and Row: New York, 1971.
(46) Keki, S.; Deak, G.; Kuki, A.; Zsuga, M. *Polymer* **1998**, *39*, 6053.
(47) Brandrup, J.; Immergut, H. E. *Polymer Handbook*; Wiley-Interscience: New York, 1975.
(48) Talingting, M. R.; Munk, P.; Webber, S. E.; Tuzar, Z. *Macromolecules* **1999**, *32*, 1593.
(49) Munk, P. In *Solvents and Self-Organization of Polymers*; Webber, S. E., et al., Eds.; Kluwer Academic Publishers: Dordrecht, The Netherlands, 1996; pp 374−375.
(50) Chang, Y.; Lee, S. C.; Kim, T. K.; Kim, C.; Reeves, S. D.; Allcock, H. R. *Macromolecules* **2001**, *34*, 269.

MA021618R